

ANALYSIS OF THE PRESSURE PROFILE IN A TUBULAR COMBUSTION CHAMBER USING FINITE VOLUME METHOD TO OBTAIN THE DISCHARGES FLOW COEFFICIENTS

Giuliano Gardolinski Venson

Federal University of Minas Gerais
Mechanical Engineering Department
Belo Horizonte, Minas Gerais, Brazil
venson@ufmg.br

Ramón Molina Valle

Federal University of Minas Gerais
Mechanical Engineering Department
Belo Horizonte, Minas Gerais, Brazil
ramon@demec.ufmg.br

Gilberto Augusto Amado Moreira

Federal University of Minas Gerais
Mechanical Engineering Department
Belo Horizonte, Minas Gerais, Brazil
gilbertomoreira@yahoo.com.br

José Eduardo Mautone Barros

Federal Center Technological Education of Minas Gerais
High School Department
Belo Horizonte, Minas Gerais, Brazil
mautone@des.cefetmg.br

ABSTRACT

This work presents the modeling and simulation of the air flow in a tubular combustion chamber, using a commercial computer assisted software based in the finite volume method. The flow is shaped using the Navier-Stokes equations through the SST (Shear Stress Transport) turbulence model. The goal of the modeling is to achieve the pressure profile along the chamber, where the air flow is separated through diffusers and some radial orifices. The discharges coefficients of each characteristic section, and the percentage of air that crosses each section, are calculated using the modified Bernoulli equation. The coefficients calculated through the simulated pressure values are compared with experimental data to validate the modeling process.

INTRODUCTION

To evaluate the quality of a combustion process, it's necessary to know the amount of air that directly act in the combustion. This amount of air is directly related with the burner by-pass ratio, that corresponds the portion of air that is deviated from its primary zone in relation to the not deviated portion. The primary zone of the burner is where the combustion process occurs. This work presents a methodology for a burner by-pass determination using the concepts of discharge flow coefficients. The burner consists in a tubular combustion chamber, designed to operate with gaseous fuels. The coefficients are calculated through the pressure drop values in the chamber, considering different areas for air flow.

The values are achieved through the pressure profile obtained in computational air flow simulations, using a commercial software based on the finite volume method. The air flow is shaped through the SST turbulence model, based on Navier-Stokes equations.

Combustion Chamber

A combustion chamber consists of a thermal equipment where the mixture air-fuel is burned. The chemical energy from the fuel is transformed into thermal energy to the air flow by the combustion process. The dimensions of the combustion chamber in case are shown at Figure 1 and the main constituent parts at Figure 2.

In this chamber the deviation of primary air is accomplished through a diffuser positioned in front of the primary orifice, presented in Figure 2. The portion of air that is deviated from the primary zone is again introduced into the flame tube through the secondary and tertiary orifices, also shown in Figure 2. The main functions of this portion of air are to cool down the flame tube wall and act as a thermal insulator.

The flame stabilization system adopted in the combustion chamber is a "buff-body" type, positioned in the flow direction after the primary orifice. The fuel injector is located inside the bluff-body, at the combustion chamber center line, and could be used only for gaseous fuel injection.

The flame stabilization system also generates a recirculation zone, guaranteeing a mixture ratio between the air flow and the fuel flow.

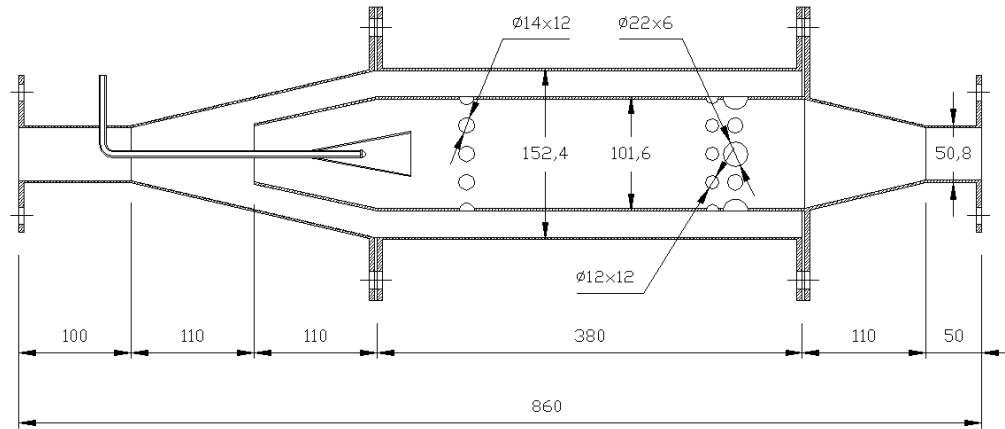


Figure 1 - Combustion Chamber Dimension (in mm)

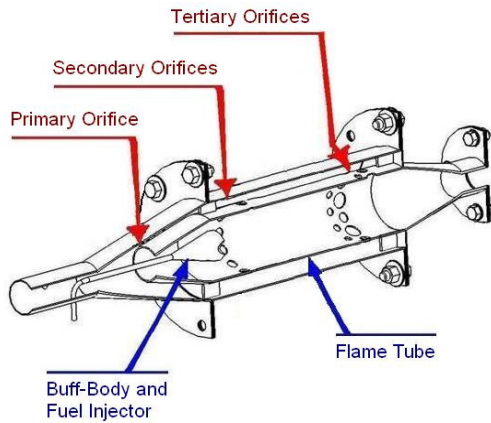


Figure 2 - Combustion Chamber Main Parts

Turbulent Flow Modeling

Turbulent flow can be defined as the viscous flow in which fluid particles move in a random and chaotic way within the flow field. The designation of viscous flow refers to a real fluid flow regardless of its viscosity value. Speed and all other fluid properties changes continuously, with strong concurrent molecular mixing between adjacent fluid layers. Specific models are used to predict such effects in complex fluid flows, where the presence of turbulence is certain (Sklavounos e Rigas, 2004).

The models are based on the Navier-Stokes equations, classified as Reynolds stress models or eddy-viscosity models. The stress models had appeared in 1895 when Osborne Reynolds introduced the Navier-Stokes average equations. By that time these models were very limited and could be applied only in particular problems or with similar geometric configurations to some previously studied. That would be improper for flows above complex geometries (Chatot, 2002).

By the computers advance after World War II (50' of past century), the 2nd order models or eddy viscosity models had appeared.

These models suggested that turbulence consists of small eddies which are continuously generated and dissipated, and where the Reynolds stresses are assumed to be proportional to mean velocity gradients. The simple zero-equation model plus to the more complex two-equation turbulence models comprise the family of eddy-viscosity models (Sklavounos e Rigas, 2004). The models commonly applied in computational flow simulations are k- ϵ , k- ω and SST turbulence models

The SST Turbulence Model

One of the main problems in turbulence modeling is the accurate prediction of flow separation from a smooth surface, existing in many technical applications both for external and internal flows. Models based on the ϵ -equation predicts the onset of separation too late and under-predict the amount of separation later on. The SST, Shear Stress Transport, turbulence model was developed to overcome deficiencies in the standard k- ϵ model and it's considered more integrated compared with k- ω and recommended for higher accuracy boundary layer simulation (Sklavounos e Rigas, 2004).

The k- ω model assumes that the turbulence viscosity is linked to the turbulence kinetic energy and turbulent frequency by the relation:

$$\mu_T = \frac{\rho k}{\omega} \quad (1)$$

Where ρ is specific mass of the fluid in kg/m³, k is the turbulent kinetic energy per unit of mass in m²/s² and ω is the turbulent frequency in Hz.

It solves two transport equations, one for the turbulent kinetic energy k and one for the turbulent frequency ω , respectively:

$$\frac{\partial(\rho k)}{\partial t} + \nabla(\rho U k) = \nabla \left[\left(\mu + \frac{\mu_T}{\sigma_k} \right) \nabla k \right] + P_k - \beta' \rho k \omega \quad (2)$$

$$\frac{\partial(\rho\omega)}{\partial t} + \nabla(\rho U\omega) = \nabla \left[\left(\mu + \frac{\mu_T}{\sigma_\omega} \right) \nabla \omega \right] + \frac{\alpha\omega P_k}{k} - \beta\rho\omega^2 \quad (3)$$

Where U is velocity vector in m/s, μ is the dynamic viscosity in kg/m.s, σ_k e σ_ω are dimensionless constants equal to 1.0 and 1.3 respectively, P_k is the turbulence production due to viscous and buoyancy forces in kg/m.s³, which is modeled using Equation (4), and α , β , β' are dimensionless constants equal to 0.56, 0.075 and 0.09 respectively.

$$P_k = \mu_T \nabla U (\nabla U + \nabla U^T) - \frac{2}{3} (\nabla U) (3\mu_T \nabla U + \rho k) + P_{kb} \quad (4)$$

Both k- ϵ and k- ω turbulence models do not consider the transport of the turbulent shear stress. By that, it results in an over prediction of the eddy-viscosity. The proper transport behavior can be obtained by a limiter to the formulation of the eddy-viscosity:

$$\nu_T = \frac{\alpha_1 k}{\max(\alpha_1 \omega S F)} \quad (5)$$

Where ν_T is the turbulence kinematic viscosity in m²/s, α_1 is a dimensionless constant of turbulence model, F is a blending function of the distance to the nearest wall and the flow variables k and ω which restricts the limiter to the wall boundary layer and S is an invariant measure of the strain rate.

Modified Bernoulli Equation

Bernoulli's Equation is used to modulate the mass flow that crosses depression elements generators. This equation could be applied only in incompressible flows, where the Mach number does not overcome the value of 0.3. To design these elements, the discharge flow coefficient is listed in function of the air flow inlet and outlet area ratio.

The same equation can be applied to determine the discharge flow coefficient of a characteristic area section if the mass flow across this section are known. The modified Bernoulli equation, used in depression elements, is presented in Delm e (1983):

$$\dot{m} = C_d E A_2 \sqrt{2\Delta p \rho} \quad (6)$$

Where \dot{m} is the mass flow in kg/s, C_d is the discharge flow coefficients, E is the dimensionless velocity coefficient, calculated through the flow areas ratio, A_2 is the throat flow area in m² and Δp is the static pressure drop across the depressive element in Pa.

Considering that inlet and outlet chamber flow areas are equal and the mass flow across the chamber is known, the discharge flow coefficient is expressed in the form:

$$C_d = \frac{\dot{m}}{A_{REF} \sqrt{2\Delta p \rho}} \quad (7)$$

DISCHARGE FLOW COEFFICIENTS CALCULATION METHOD

The discharges flow coefficients of primary, secondary and tertiary orifices are calculated from differential method. It uses the same method used in electrical systems for determination of the equivalent electrical resistance when the resistances are connected in parallel, according to the relation:

$$\frac{1}{R_{eq}} = \frac{1}{R_1} + \frac{1}{R_2} + \frac{1}{R_3} + \dots + \frac{1}{R_n} \quad (8)$$

As function of the discharges flow coefficients of the primary, secondary and tertiary orifices, the Eq. (8) rewrites in the following form:

$$\frac{1}{C_{deq}} = \frac{1}{C_{d1}} + \frac{1}{C_{d2}} + \frac{1}{C_{d3}} \quad (9)$$

Where C_{deq} is the equivalent discharge flow coefficient, C_{d1} , C_{d2} and C_{d3} are the discharge flow coefficients of the primary, secondary and tertiary orifices respectively.

The practical method to obtain these coefficients consists in an alternated blockade of the air flow orifices. When one or more orifices are blocked, the respective discharge flow coefficient becomes zero, generating different equivalent discharge flow coefficient for each tried combination.

An equation system is used to calculate the discharge flow coefficient of each set of orifices. With the coefficients relation is possible to calculate the percentage of air that crosses each section, and consequently the by-pass ratio of the combustion chamber.

PRESSURE PROFILE MODELING

Boundary Conditions of Air Flow Simulation

The air flow simulations along the combustion chamber are made using the commercial software CFX 9. Inlet conditions are: air mass flow, temperature and absolute pressure. The outlet condition is the same air mass flow. The mass flow adopted is 0.085 kg/s, temperature 298 K and absolute pressure of 101.3 kPa. The chosen turbulence model is the SST, without alterations in the turbulence constants.

The combustion chamber volume considered for analysis relates to its real geometry. To evaluate the behavior of the discharge coefficient of the chamber as function of the different air flow areas, 4 (four) simulations had been made, which are described in Table 1. In the presented simulations, the blockades of the orifices were made changing the combustion chamber basic drawing.

Table 1 - Simulations Description

number	description	equivalent discharge flow coefficient equation
1	all orifices open	$\frac{1}{C_{d1}} + \frac{1}{C_{d2}} + \frac{1}{C_{d3}}$
2	only primary orifice open	$\frac{1}{C_{d1}}$
3	primary and secondary orifices open	$\frac{1}{C_{d1}} + \frac{1}{C_{d2}}$
4	primary and tertiary orifices open	$\frac{1}{C_{d1}} + \frac{1}{C_{d3}}$

Generated Volume Mesh

In the air flow simulations the same volume mesh configurations were used. The Figure 3 presents the external aspect of the volume mesh generated for all simulations. The mesh details, generated automatically by the software, are shown in Table 2.



Figure 3 - Combustion Chamber Volume Mesh

Table 2 - Volume Mesh Details

parameter	simulation number			
	1	2	3	4
number of nodes	78,575	44,250	55,606	66,569
number of elements	408,630	225,484	285,535	345,426
number of tetrahedras	408,630	225,484	285,535	345,426
number of faces	35,580	22,342	26,764	30,262

Simulations Results

The pressure profiles along the combustion chamber, with its the flow simulations description, are shown in Figure 4. The total pressure profile obtained considering all orifices opened is represented in Figure 5.

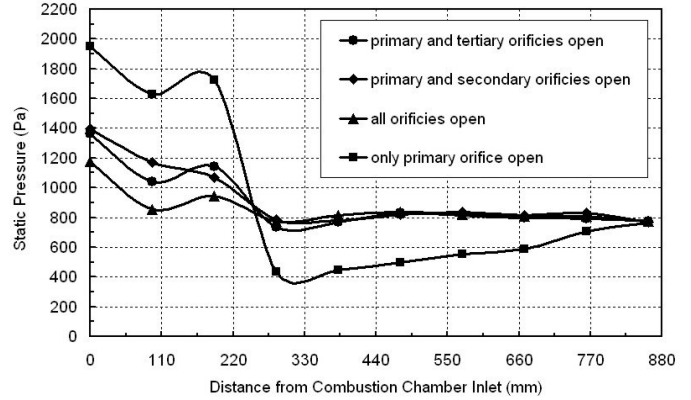


Figure 4 - Pressures Profiles Obtained

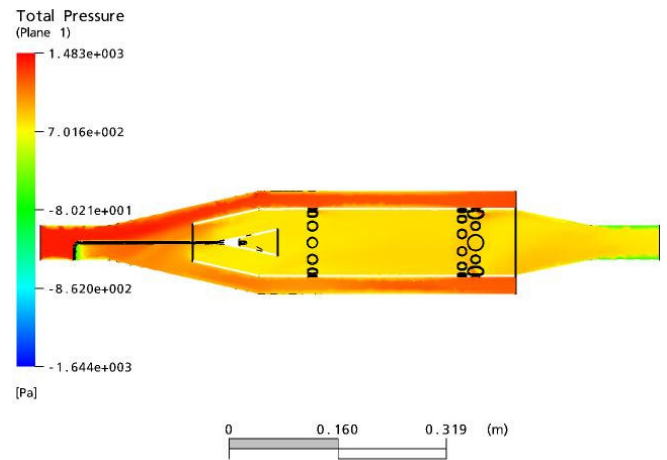


Figure 5 - Chamber Total Pressure Profile

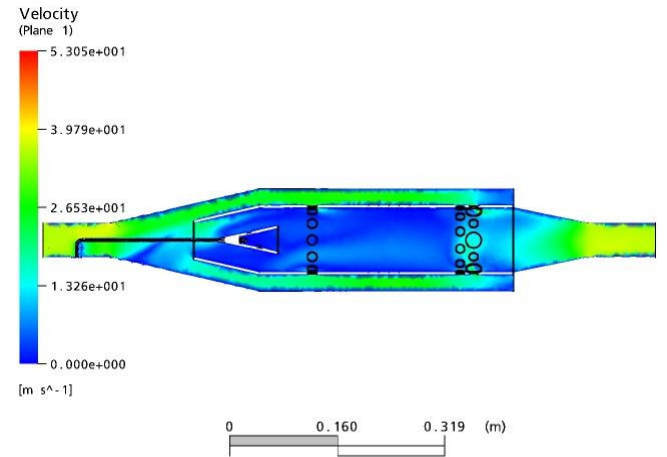


Figure 6 - Chamber Velocity Profile

With the air flow velocity profile showed in Figure 6, it verifies that the maximum value is approximately 40 m/s, that corresponds a Mach number of 0.12. As this value is lower than 0.3, the Equation (7) could be applied.

Combustion Chamber Discharge Flow Coefficients

The equivalent discharges flow coefficients are calculated through the pressure drop values and the total flow area, which are calculated through the chamber dimensions shown in Figure 1. The results are presented at Table 3.

Table 3 - Simulated Equivalent Discharge Coefficients

number	mass flow (kg/s)	total flow area (m ²)	pressure drop (Pa)	equivalent discharge flow coefficient
1	0.085	0.00844	402	0.34078
2	0.085	0.00203	1,190	0.89850
3	0.085	0.00387	627	0.67437
4	0.085	0.00659	585	0.38993

The flow coefficients discharges of each chamber orifice are obtained through the calculated equivalent values and its respective equation, showed at Table 1. The values of each of those coefficients are presented at Table 4. Table 5 shows the chamber by-pass ratio calculated through the primary, secondary and tertiary discharges flow coefficients.

Table 4 - Simulated Chamber Discharges Flow Coefficients

number	1/C _{deq}	1/C ₁	1/C ₂	1/C ₃
1	2.93447	1.11297	0.36990	1.45160
2	1.11297	1.11297	-	-
3	1.48287	1.11297	0.36990	-
4	2.56457	1.11297	-	1.45160

Table 5 - Flow Percentage Based in Simulations Results

chamber orifices	1/C _{deq}	flow percentage
all orifices	2.93447	100.00%
primary	1.11297	37.93%
secondary	0.36990	12.61%
tertiary	1.45160	49.47%
by-pass ratio	5:3	

The air flow Reynolds number, calculated through the mass flow and chamber inlet area, are 124.000, proving that the flow is at turbulent regime.

Modeling Validation

The simulations results were compared with experimental data, through the instrumented combustion chamber shown in Figure 7.

In the experimental stand, a differential pressure sensor was fixed at chamber inlet and outlet position, as shown in Figure 7. The sensor used was a MPX-5010 DP, with range from 0 to 10 kPa and 100 uncertainty of 100 Pa. The mass flow was obtained from the pressure drop in an orifice plate positioned before the combustion chamber. A centrifugal blower was used to produce the airflow into the chamber. The experimental results are shown at Tables 6 to 8.

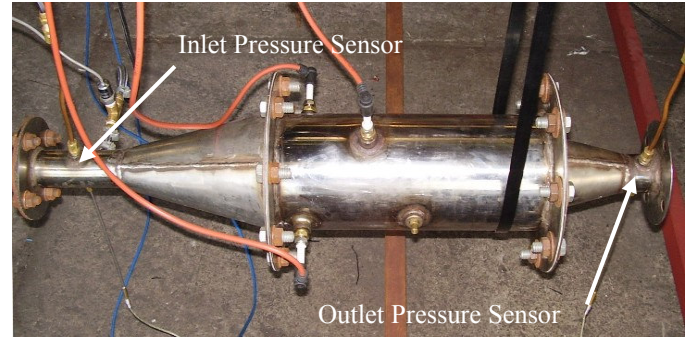


Figure 7 - Combustion Chamber

Table 6 - Experimental Equivalent Discharge Coefficients

number	mass flow (kg/s)	total flow area (m ²)	pressure drop (Pa)	equivalent discharge flow coefficient
1	0.085	0.00844	499	0.31508
2	0.083	0.00203	1,392	0.76370
3	0.084	0.00387	767	0.58572
4	0.084	0.00659	673	0.36024

Table 7 - Experimental Chamber Discharges Flow Coefficients

number	1/C _{deq}	1/C ₁	1/C ₂	1/C ₃
1	3.17382	1.30942	0.39787	1.46654
2	1.30942	1.30942	-	-
3	1.70729	1.30942	0.39787	-
4	2.77596	1.30942	-	1.46654

Table 8 - Flow Percentage Based in Experimental Results

chamber orifices	1/C _{deq}	flow percentage
all orifices	3.17382	100.00%
primary	1.30942	41.26%
secondary	0.39787	12.54%
tertiary	1.46654	46.21%
by-pass ratio	3:2	

The criteria used to validate the simulations are the comparison between the simulated and experimental results for pressure drop values and flow percentage, of each chamber characteristic section. The final results are presented at Tables 9 and 10.

Table 9 - Pressure Drop Comparison

number	pressure drop		deviation
	experimental	simulated	
1	499	402	- 19.38%
2	1,392	1,190	- 14.51%
3	767	627	- 18.25%
4	673	585	- 13.12%

Table 10 - Flow Percentage Comparison

chamber orifices	flow percentage		deviation
	experimental	simulated	
primary	41.26%	37.93%	- 7.85%
secondary	12.54%	12.61%	+ 0.24%
tertiary	46.21%	49.47%	+ 6.92%
by-pass ratio	3:2	5:3	+ 11.11%

CONCLUSIONS

The air flow computational simulation along the combustion chamber using the SST turbulence model presented satisfactory results. The maximum deviation of the percentage of air flow in the characteristics sections are 8% (eight percent) lower than the same values calculated from experimental data.

The simulated static pressure drops values presented the same physical behavior than the experimental values. The higher pressure drop in the chamber was obtained with the blockade of the secondary and tertiary orifices. However, with all orifices open, it was obtained the lower pressure drop value. This fact is associated directly with the flow area, since higher areas cause a lower pressure drop. The pressure drop values, obtained in each simulation, are also close to the obtained experimentally, presenting maximum deviation of 19% lower (nineteen percent).

The validation of the results allows extending the methodology to analyze the flow behavior inside the chamber, visualizing stagnation and recirculation zones.

ACKNOWLEDGMENTS

To the Fundação de Amparo à Pesquisa do Estado de Minas Gerais, through the FAPEMIG/FINEIP EDT 1647/04 project.

REFERENCES

ANSYS Company, 2003. "CFX Solver Theory Manual". Oxfordshire: CFX.

Chatot, J. J., 2002. "Computational Aerodynamics and Fluid Dynamics: An Introduction". New York: Springer. 186 p.

Delmée, G. J., 1983. "Manual de Medição de Vazão". São Paulo: Editora Edgard Blucher. 474p.

Maliska, C. R., 1995. "Transferência de Calor e Mecânica dos Fluidos Computacional". Rio de Janeiro: Editora Livros Técnicos e Científicos S/A.

Souza, R. A. "Análise de Desempenho de uma Câmara de Combustão para Aplicação em uma Microturbina à Gás". Belo Horizonte: Escola de Engenharia da UFMG, 2005. 60p.

Sklavounos S., Rigas F., 2004. "Validation of Turbulence Models in Heavy Gas Dispersion Over Obstacles". Journal of Hazardous Materials, A108 9-20. Elsevier. pp. 12-13.